Optimisation of the FeMn and ZnO Production from Spent Pyrolised Primary Batteries – Feasibility of a DC-Submerged Arc Furnace Process

Ricardo Sánchez-Alvarado, Bernd Friedrich

In the present work the feasibility to produce a Fe-Mn-alloy and a ZnO-concentrate from spent pyrolised primary batteries has been investigated based on fundamental research, already reported in „World of Metallurgy" – ERZMETALL 1/2007. Through a carbothermic reduction in a Direct Current Submerged Arc Furnace process (DC-SAF) at IME Aachen, several laboratory-scale as well as semi-pilot scale tests were conducted with three different slag-compositions using solid- and hollow-electrode technique. The process was theoretically modelled with the thermochemical package FactSage 5.3.1. The effect of the process parameters temperature, slag composition and carbon addition were analysed. The results show that it is possible to recycle spent primary batteries through the submerged arc route to obtain a Fe-Mn-alloy with a ratio Mn/Fe > 1 and a ZnO concentrate as a separated product, reaching recycling quotes for Mn between 44 and 62 %, for Fe between 56 and 96 % and for zinc of more than 90 %.

Keywords:

Recycling efficiency – Direct Current Submerged Arc Furnace (DC-SAF) – Spent primary batteries, – Carbothermic reduction – Ferromanganese – Zinc

Optimierung der Ferromangan- und Zinkoxid-Herstellung aus pyrolisiertem Primärbatterieschrott – Durchführbarkeit eines Gleichstrom-Lichtbogenofen-SAF-Prozesses

In der vorliegenden Arbeit wird die Erzeugung einer Fe-Mn-Legierung und eines ZnO-Konzentrates aus pyrolisiertem Primärbatterieschrott untersucht, basierend auf den in „World of Metallurgy – ERZMETALL" Heft 1/2007 berichteten Grundlagenforschungen. Durch karbothermische Reduktion in einem Gleichstrom-Lichtbogenofen des IME der RWTH Aachen konnte im Labormaßstab wie auch in Pilot-Versuchen die prinzipielle Machbarkeit anhand von drei verschiedenen Schlackenzusammensetzungen nachgewiesen werden. Parallel wurde der Prozess mittels thermochemischer Rechnungen (Software FactSage 5.3.1) theoretisch modelliert. Ein signifikanter Einfluss von verschiedenen Prozess-Parametern wie Temperatur, Schlackenzusammensetzung und Kohlenstoffzugabe konnte aufgezeigt werden. Die Ergebnisse zeigen, dass eine Fe-Mn-Legierung mit Mn/Fe > 1 und ein ZnO-Konzentrat als getrennte Produkte gewonnen und Recyclingeffizienzen für Mn zwischen 44 und 62 %, für Fe zwischen 56 und 96 % und für Zink mit mehr als 90 % erreicht werden können.

Schlüsselwörter:

Recyclingeffizienz – Gleichstrom-Lichtbogenofen – Primärbatterien – karbothermische Reduktion – Ferromangan – Zink

Optimisation de la production de ferromanganèse et d'oxyde de zinc sur la base des ferrailles primaires des batteries – praticabilité d'un processus SAF dans un four à arc au courant continu

Optimización de la producción de ferromanganeso y oxido de zinc de baterías primarias pirolizadas desgastadas – Factibilidad de un proceso de arco sumergido de CD

1 Background and aim of the project

1.1 Market and scrap volume

In the last 30 years the amount of domestic refuse and industrial waste has continuously risen. The growth of world population and demand for a higher standard of life increase the consumption of raw materials and waste produced. The large amount of waste is a true problem everywhere. The storage capacity of landfills and special waste dumpsites is limited. The most common primary batteries in use today are the zinc-carbon and the alkaline-manganese battery systems. Together, they constitute more than 80 % by weight of the total consumer battery market in Europe, exemplary the amount of sold batteries for Germany

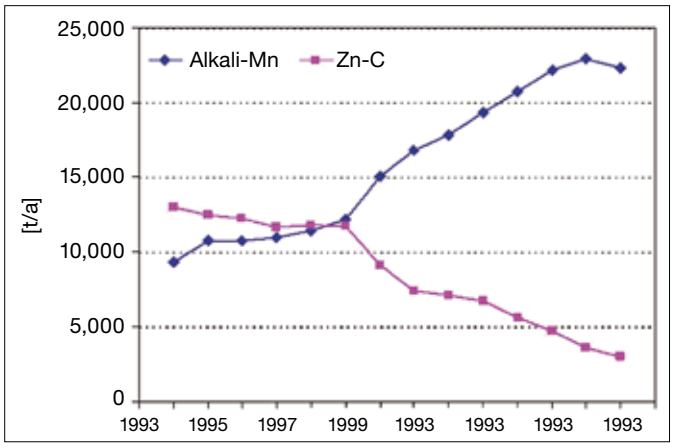

Fig. 1: Primary battery sales in Germany [2]

is given in Figure 1. In the last six years the recycling of batteries reached an increment in the collection rate from 19 % (1999) to 82 % (2005). In the year 2005, the quantity of collected batteries in Europe reached 12,263 tons [1].

In July 2006, the European Parliament and the EU Council of Ministers agreed on a compromise to revise the 1991 directive on batteries and accumulators. The new directive provides (inter alia) for collecting and recycling targets to be reached by 2016 at the latest. It has been set that any process for the recycling of batteries will be obliged to reach a recycling efficiency of 65 % by average weight for lead-acid batteries and 75 % for nickel-cadmium and 50 % for other battery types.

Because of their valuable element content primary batteries are among the materials, which should be recycled. Worldwide consumption of primary batteries rises annually. They contain an important quantity of metals, which can be recovered with less energy consumption through a recycling process than would be necessary for winning these metals from the ores. The range of chemical composition for unused primary batteries is given in Table 1.

Table 1: Zinc-carbon and alkaline-manganese battery composition range [wt.-%] [3]

Battery component	Zn-C	Alkaline-Mn
Zn	16.4 - 28.6	5.4 - 17.5
ZnO	0.3 - 0.4	0 - 0.6
Hg_{total}	max. 0.04	max. 0.04
MnO_2	22 - 34	17 - 38
organics	7 - 10.6	3.0 - 5.0
Fe	14 - 21	15 - 26
Cu	0 - 0.2	1.0 - 3.0
miscellaneous parts	4.0 - 13.0	4.0 - 11.0
electrolyte	14 - 23	5.0 - 16.0

1.2 Metallurgical challenges

1.2.1 Manganese

The treatment of primary batteries through a standard SAF-process alone is not capable of attaining a sufficient manganese recovery. In fact, in all recycling processes for primary batteries manganese is found in high proportions in the slag, resulting in an insufficient metal recycling efficiency and also economic losses. Thus, the SAF-route requires modifications in order to improve this situation. As manganese in a FeMn30 alloy has a vapour pressure at least 250 times higher than iron at 1600 °C, the process temperature has to be as low as possible in order to produce a Fe-Mn alloy. A second requirement is a suitable slag system serving the following characteristics at process conditions in order to achieve a high manganese recovery yield:

- Molten condition (sufficient superheat) at process temperatures about 1500 °C;
- Low vapour pressures of the slag components;
- Manganese solubility significantly less than 20 weight-%;
- Low viscosity to allow metal drop settling;
- High density difference between the metal and slag phase.

A slag system that fulfils these requirements has been found to be:

- CaO = 56.3 %, SiO_2 = 43.7 %
- CaO = 46.7 %, SiO_2 = 38.3 %, Al_2O_3 = 15.0 %
- CaO = 45.7 %, SiO_2 = 37.3 %, Al_2O_3 = 14.0 %, MgO = 3.0 %.

These investigations have been reported in a prior article [4].

1.2.2 Zinc

Metallic zinc is one of the most important components in batteries, being used as an anode due to its electrochemical features and relative low costs. For alkaline cells, zinc is used in powder form and of high purity (99.85 to 99.00 %). Usually it is produced by electrowinning or distillation. On the other hand, there are limited natural sources for zinc on earth. Data from the US Bureau of Mines informs that the worldwide zinc mineral supplies will be exhausted in about 30 years, making it the most rare commodity metal in the world. Compared to its other uses, as in alloy and protection of steelwork, the amount of zinc being used in the production of batteries is small. So a battery contains at least approximately 16 % of Zn, which means 18 % of world production [5].

1.2.3 Aim of the present work

In the new battery directive for the European recyclers (publication September 2006) battery recycling targets have been for the first time concretised in data. Apart from the requirement to collect portable batteries and accumulators (defined as collection rates) the intensification of material recycling is demanded, respectively in article 19 minimum recovery quotas are defined (so called Recycling Efficiencies). For the primary battery systems Zn-C and Alkali-Mn any recycling process must recover at least 50 % by average of the battery scrap weight. Still open is the question about the kind of products to count for such recycling efficiencies. Recently a first analysis about technical recycling quotas in a one step SAF-treatment process of spent primary batteries was done [6] (Figure 2). The presented metal recovery values are the minimum to overcome the efficiency requirements, if the calculation is based on recovered metal products.

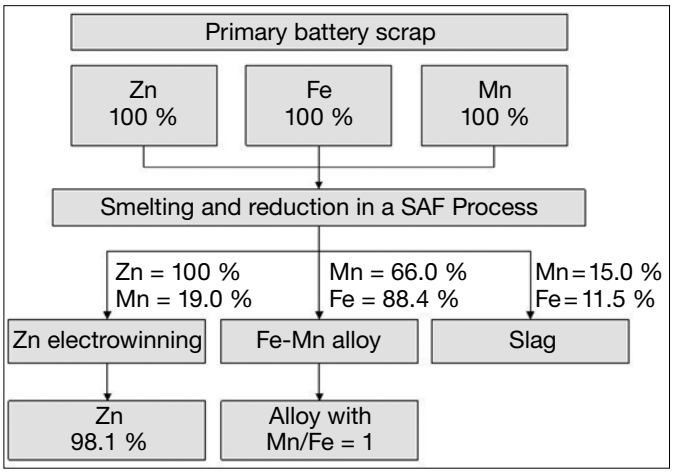

Fig. 2: Proposed metal-recoveries in a SAF-process treating spent primary batteries to reach a metallic recovery of > 50 % [6]

The present experimental work focuses on the treatment of spent primary batteries using the DC-SAF-route, a carbothermic process where the contained manganese- and zinc oxide is reduced. Together with the steel of the battery can, manganese is recovered to some extend forming a Fe-Mn alloy, while the zinc oxide is reduced, Zinc is evaporated and oxidized again above the burden and recovered as ZnO.

2 Chemical reactions during reductive smelting

In spent primary batteries, the products of the electrochemical reactions are mainly zinc- and manganese-oxides. These oxides must be decomposed to recover the contained metals, e.g. by carbothermic reduction, and the formation of manganese and zinc becomes possible. Because of the chemistry of primary batteries, the proposed DC-SAF recycling process aims on the formation of a marketable ferromanganese alloy as well as the recovery of Zinc as metal or as ZnO-concentrate. The carbon contained in primary batteries is in graphite form and in the pyrometallurgical process has to be used as much as possible as reductant. This should improve the recycling efficiency by diminution of the total needed carbon in the process. The iron content is mainly presented in a metallic form (can of the batteries); hence it must not be reduced; only melted in the recycling process. Its recovery expectations are above 90 %. In this work, the reaction mechanism of this process is evaluated.

2.1 Manganese reduction from its oxides

Ferromanganese can be produced either in blast or electric arc furnaces from ores containing both manganese and iron oxides. It is reported that the ore needs to have a Mn/Fe-weight percentage ratio of at least six in order to ensure both satisfying manganese recovery and grade. [4, 5]. Electric arc furnace smelting is today more popular than blast furnace smelting. Electric arc furnaces are very flexible as they can be used to produce either ferromanganese or silicomanganese. At small production capacities, they are also economic provided that regular supplies of electric power are available at reasonably low cost. There are two smelting methods used for electric arc furnaces. The waste slag process aims at maximising the recovery of manganese in metallic form and produces a discardable slag containing "only" 15 to 20 % manganese, while the manganese-rich slag process aims at producing a slag with 30 to 40 % manganese, being feed for the silicomanganese production. The latter is favoured since it leads to lower power consumption, increased furnace productivity, reduced coke requirements and operates at lower temperatures. Thus it reduces manganese vaporization losses and the diminution of pollution issues [7, 8].

As in all smelting processes, the metallurgical reactions in the electric ferromanganese furnace are complex and variable. The major reactions, however, can be expressed as simple chemical equations; the order varies to some extent, depending on the operating conditions of the furnace. For example, with good operating conditions and a burden of high porosity, which allows a good distribution of the reduction gas through the mix, a considerable degree of reduction of the higher oxides with carbon monoxide takes place even in the solid state. This is reflected in higher carbon dioxide concentrations of the furnace gas and results in a lower requirement of electric power for smelting. In most oxide ores and also in spent primary batteries manganese is present mainly as the tetravalent ion. Using carbon and carbon monoxide, the reactions on the way to manganese metal start with the prereduction of manganese dioxide, may be expressed simply as:

$$MnO_2 + C \rightarrow MnO + CO \quad (1)$$

$$MnO_2 + CO \rightarrow MnO + CO_2 \quad (2)$$

The reduction with solid carbon is slightly endothermic, while the reduction with carbon monoxide is strongly exothermic. Parallel to that higher manganese oxides easily dissociate at elevated temperatures, the prereduction may be also expressed as a decomposition:

$$4MnO_2 \rightarrow 2Mn_2O_3 + O_2 \quad (3)$$

$$6Mn_2O_3 \rightarrow 4Mn_3O_4 + O_2 \quad (4)$$

$$2Mn_3O_4 \rightarrow 6MnO + O_2 \quad (5)$$

Manganic oxide (Mn_2O_3) dissociates to manganous oxide at 950 °C. Manganous oxide (Mn_3O_4) is converted to manganese monoxide by the time the furnace's smelting temperature of 1200 °C to 1400 °C is reached. The reaction of manganese monoxide with solid carbon produces metallic manganese and manganese carbide parallel. Thermochemically, MnO cannot be reduced by CO at reasonable temperatures. Such the reduction mechanism of MnO is analogous to that of FeO [9].

$$MnO + C \rightarrow Mn + CO \quad (6)$$

$$6MnO + 8C \rightarrow 2Mn_3C + 6CO \quad (7)$$

Liberated oxygen combines with carbon to form carbon monoxide. It also combines with carbon monoxide to form carbon dioxide. Under favourable operating conditions, higher manganese oxides are reduced to lower oxides with carbon monoxide (partial-reduction of higher manganese-oxides) These reactions may be expressed as follows:

$$2MnO_2 + CO \rightarrow MnO_2O_3 + CO_2 \quad (8)$$

$$3Mn_2O_3 + CO \rightarrow 2Mn_3O_4 + CO_2 \quad (9)$$

$$Mn_3O_4 + CO \rightarrow 3MnO + CO_2 \quad (10)$$

"Direct" reduction process is strongly endothermic and imposes a high energy input to the furnace. In the DC-SAF process, direct reduction takes place in the hottest region below the electrode. Carbon dioxide combines with carbon to regenerate carbon monoxide, known as Boudouard reaction, which is only fast enough above 1000 °C to comply with the generation of carbon dioxide. The "indirect" reduction reactions are exothermic. In the DC-SAF process, indirect reduction takes place in the cooler overlying charge (burden), which is both heated and reduced by the rising carbon monoxide. At temperatures below 1000 °C, the reduction process is known as "indirect reduction" and proceeds according to equation (8) to (10). In the case for manganese oxides it is only a pre-reduction of the higher oxides. Any carbon dioxide produced by this reaction leaves the furnace without undergoing further interaction with carbon.

2.2 Zinc reduction from its oxides

Today a large amount of zinc metal is industrially recovered from the EAF-dust by the carbothermic reduction method, mainly in Waelz-kiln or comparable processes like rotary hearth or multiple hearth. These methods producing a zinc oxide-concentrate have the advantages of process simplicity and easy upscaling for large-scale operation. But for the metallic recovery or the treatment in an electric arc furnace only limited literature can be found. The recovery of zinc metal from zinc oxide or from EAF-dusts through a carbothermic reduction was found to be feasible by [10]. The metal oxide reduction with CO takes place at temperatures higher than 1350 ºC according to the following main reactions:

$$ZnO + CO \rightarrow Zn + CO_2 \quad (11)$$

In direct contact with solid carbon the reduction of ZnO takes place at around 900 °C according to (12) and above the slag bath, the metal vapour is reoxidized with secondary air, and the offgas is post-combusted (13):

$$ZnO + C \rightarrow Zn + CO \quad (12)$$

$$Zn + ½\ O_2 \rightarrow ZnO \quad (13)$$

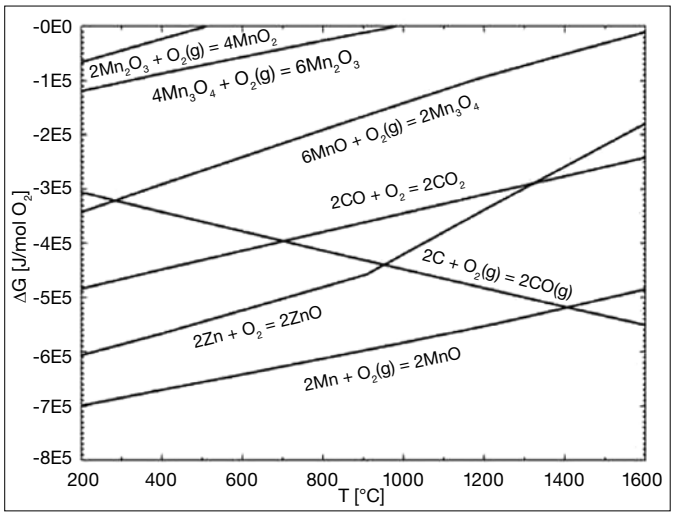

Fig. 3: Ellingham diagram of the metallic oxides contained in spent primary batteries calculated in Fact Sage 5.3.1 (standard conditions and pure substances)

Figure 3 shows the Ellingham diagram (equilibria for pure substances and standard state) for the carbothermic reduction (with solid C and CO) for the metallic oxides contained in spent primary batteries. Of course these data can give only indications or tendencies, as the metal-oxides will be partly dissolved in the liquid slag phase. This "mix-phase" leads to different activities and therefore to modified free enthalpy values.

3 Output calculation by thermochemical modelling

In the present work FactSage 5.3.1 was used for the modelling of the process. This software bases on species data and calculates data for ideal and real solutions, allowing to determine equilibria compositions of multiphase and multicomponent systems at given temperatures, pressures and initial compositions. It uses unified interaction parameters [11] for the metallic molten phase and a quasi-chemical approximation for the slag. The derived unified interaction parameter (UIPM) describes the thermodynamic behavior of components in liquid dilute alloys. This model is thermodynamically self-consistent at both infinite dilution and finite concentrations and has been used successfully for molten iron. The model describes the thermochemical properties of a system taking into account the structural ordering. In order to apply this model to a high order system, the basic quasichemical model was modified by [12]:

- providing an expression of the entropy and enthalpy, that exhibits ordering at any desired composition,
- introducing a composition-dependent energy change for the formation of pairs, and
- extending this model to ternary and multicomponent systems.

Eriksson and co-workers [13] have evaluated binary slag-subsystems with the 11 components SiO_2–CaO–Al_2O_3–FeO–MgO–MnO–Na_2O–K_2O–TiO_2–Ti_2O_3–S. But not all ternary combinations have been investigated in detail and only a few higher order systems have been studied. The model parameters for the SiO_2–CaO–Al_2O_3–MgO–MnO–K_2O system have been integrated into FACT-database. Using the equilibrium module in the software FactSage 5.3.1, equilibria computations were performed in order to analyze the effect of the temperature, slag composition and carbon addition in a SAF-process for the reprocessing of pyrolised spent primary batteries.

The result of the modelling (Figure 4) shows the amount of output materials as function of the temperature. Between 800 °C and 900 °C, the reduction of ZnO takes place in the presence of CO. Zn is evaporated instantly; the amount of Zn in the gas-phase remains constant up to 1600 °C (the reoxidation has not been included in the modelling). The formation of a liquid metallic phase begins at 1100 °C and

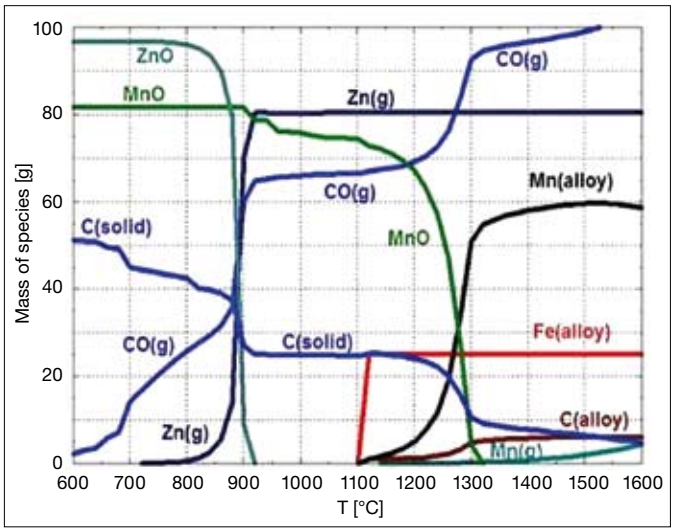

Fig. 4: Phase-equilibria in the processing of spent primary batteries through a carbothermic reduction

the Fe contained in the shells of the spent primary batteries is completely melted. Between 1100 °C and 1200 °C the dilution of manganese in the molten iron is very low. As the temperature of the liquid bath increases, the carbothermic reduction of the manganese oxides intensifies and the concentration of manganese in the alloy increases significantly. The solid C is step by step used for the reduction of the Zn- and Mn-oxides, producing CO. Partially C is dissolved in the liquid metal phase. A direct combustion only for energy generation is not considered. In the area where the C-content in the alloy increases, the major increment of manganese in the FeMn-alloy can be seen. Above 1400 °C, all MnO seems to be reduced and above 1550 °C the mass of manganese reporting to the alloy decreases as a proportion of manganese is volatilised. To avoid this situation it should be recommended to work at temperatures as low as possible (process temperature max. 1500 °C).

Such, the Fe- and Mn-content of the spent primary batteries should lead to a Fe-Mn-alloy up to 25 wt.-% Mn in the SAF process, which is due to the high iron content originating from the can material of the primary batteries in combination with the loss of manganese in the slag phase. In order to increase the manganese concentration in the FeMn-alloy to approximately 65 wt.-% (standard commodity grade), the ratio between MnO_2 and Fe in the (pre-pyrolised) spent primary batteries must be higher than nine, as the theoretical calculation in FactSage show (Figure 5). This ratio can be obtained by adding other Mn-sources like primary MnO_2 or de-ironed battery scrap to the mixture.

Figure 6 shows the effect of C-addition in equilibrium calculated with the software FactSage 5.3.1 in a DC-SAF process for the reprocessing of primary batteries. It can be seen that the amount of MnO reduced from the slag to the alloy steadily increased and then becomes constant. At this carbon addition the alloy becomes carbon-saturated and, thereafter, the amount of the saturated carbon (non-reacted) begins to increase (described as C-saturation in Figure 6). The composition of the alloy remains constant under these conditions. This is expected from a consideration of the "Gibbs Phase Rule". This system can be approximated as the four-component Fe–Mn–C–O system and where there are four phases coexisting (gas, slag, alloy, carbon) there can only be two degrees of freedom – the temperature and total pressure. The temperature and total pressure are fixed so at carbon saturation the system is invariant.

Figure 7 shows the composition of the formed alloy as function of the temperature. The manganese grade of the alloy is little affected by temperature above 1450 °C; however it also shows that the silicon content of the alloy rises with the temperature because of the partial reduction of silica from the slag. Exemplary, typical values of Si in the commercial Fe-Mn-alloy "High carbure" should not overcome 1.25 wt.-% silicon in the alloy. Hence the optimal process temperature to treat pyrolised primary batteries through carbothermic reduction seems to be 1500 °C, with this a high content of manganese is reached (about 65 wt.-%) and at the same time the concentration of silicon in the alloy remains under 1.0 wt.-%. The iron content in the alloy is about 27 wt.-%, while the carbon content in the alloy reaches 6 wt.-%.

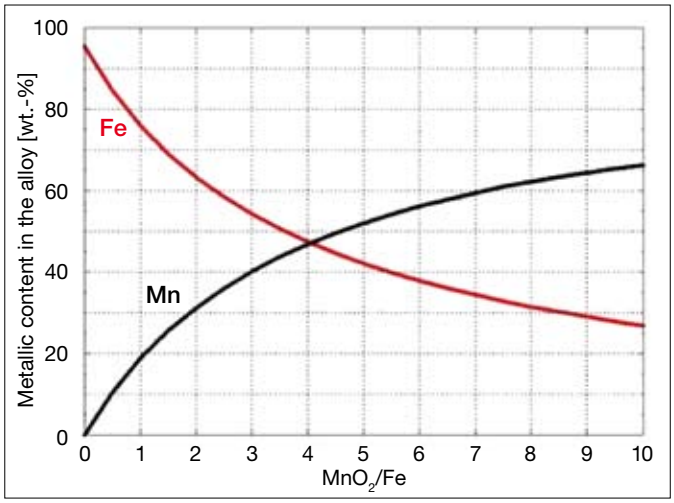

Fig. 5: Effect of the MnO_2/Fe-ratio in the feed material of an SAF-process, treating spent primary batteries at 1500 °C, calculated with FactSage 5.3.1

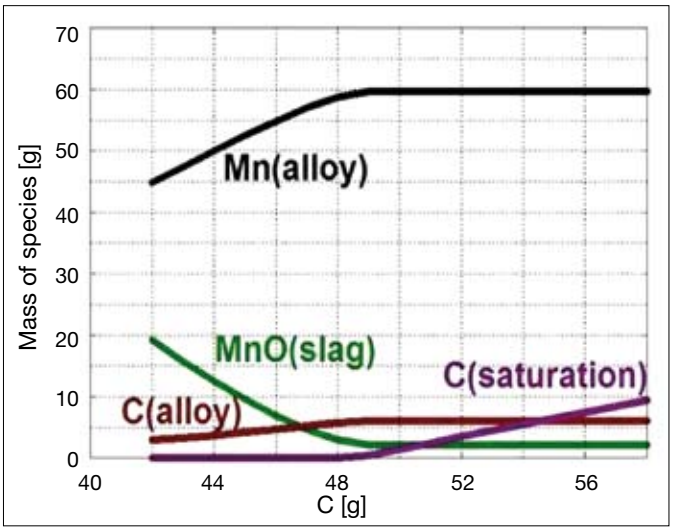

Fig. 6: Effect of the C-addition in equilibrium at 1500 °C in an SAF-process calculated in FactSage 5.3.1

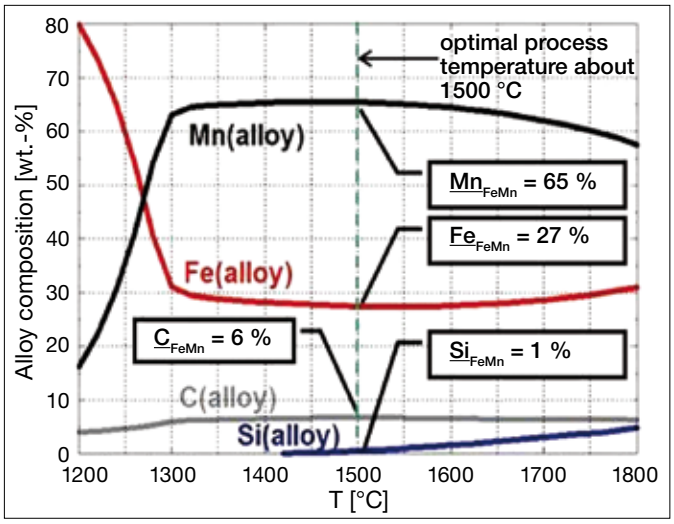

Fig. 7: Alloy composition as function of the temperature calculated in FactSage 5.3.1

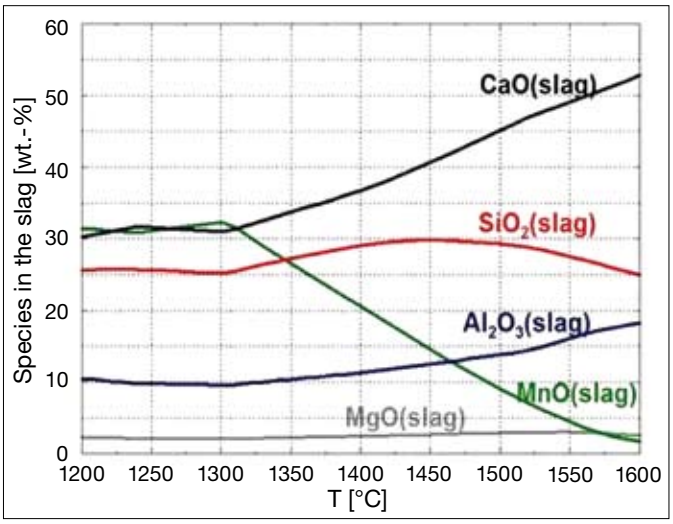

Fig. 8: Calculation of equilibrium in the slag phase for production of ferromanganese from spent primary batteries in a submerged arc furnace

Figure 8 shows the theoretical calculated equilibrium in the slag phase as function of the temperature for the production of ferromanganese from spent primary batteries in a submerged arc furnace. The basic slag system has been fixed due to investigations concerning metal/slag equilibria that have been reported in [4] and is made up from calcium-oxide, silica, alumina and magnesium-oxide. In the molten slag at 1300 °C as principal components appear CaO, SiO_2 and MnO. Between 1350 °C and 1600 °C CaO appears as the principal component in the slag. At around 1310 °C begins the diminution of the MnO concentration in the slag and it continues with a sinking tendency as the temperature increases. At 1300 °C SiO_2 is the third most abundant oxide in the molten slag, its concentration is diminished from 1470 °C to 1600 °C, this is attributed to the partial reduction of SiO_2. From 1350 °C to 1600 °C the Al_2O_3 concentration raises as the temperature increases because of the diminution of the MnO in the slag. The concentration of MgO remains more or less constant.

4 Experimental

4.1 Pre-treatment

About 2000 kg of spent primary batteries were pyrolised at temperatures between 300 and 750 °C in a shaft furnace (kindly provided by Batrec/Wimmis) in order to obtain a scrap free of electrolyte, mercury, plastics and other volatile components. After cooling, the pyrolised batteries were stored in a sealed plastic container to avoid humidity contact. Additionally about 500 kg non-pyrolised battery scrap was treated by mineral processing methods, providing a Fe-free fine powder ("black mass"). First, the batteries were fed to a hammer mill for dismantling. A magnetic separator removed the magnetic fraction and the remaining non-magnetic fraction was screened by sieving < 2.0 mm (10 mesh). This manganese-zinc-carbon-concentrate was prepared and kindly provided by Redux/Dietzenbach. The black mass powder rich in manganese oxide, zinc oxide and graphite was dried, mixed with 5 wt.-% CaO and pelletised using an aqueous solution of 15 vol.-% $NaSiO_4$. Subsequently, they were dried at 200 °C in an electrical resistance furnace for 24 hours.

As reducing agent lignite carbon with about 86 wt.-% fixed C and average particle size of 5 mm was used. Slag additive mixtures were prepared from pure oxides (CaO, SiO_2, Al_2O_3 and MgO), the corresponding weights (see chapter 4.3) of the oxide were mixed, homogenized and dried at 200 °C for 24 hours. For every experiment, the battery scrap was mixed with lignite. The carbon contained in the feed material was taken into account as reductant and added up to the calculated stoichiometric amount, needed for the reduction process. The amount of slag forming additions in all experiments was 10 wt.-% of the initial charge. Figure 9 (left) gives an impression about shape and morphology of the pre-pyrolised primary battery scrap, while Figure 9 (right) presents some "black mass"-pellets.

Fig. 9: Pyrolised spent primary batteries (top) and pelletised "black mass" (bottom)

4.2 Chemical analysis of the primary battery scrap materials

The pyrolised primary batteries and the delivered black mass were chemically analyzed. The mixture of pyrolised primary batteries contains manganese and zinc oxides, iron, remained combusted material as well as pulverized and non-pulverized graphite. The sampling procedure followed the so-called "quarter sampling method". Approximately 100 kg of pyrolised primary batteries was piled up into a conical heap, which was then intensively mechanically mixed and afterwards divided into four parts. Two diagonally opposite parts were removed from the mixture and were stored, while the remaining both quarters were mixed and homogenized again. With this new mixture the procedure was repeated. The final sample's amount used for chemical extraction was approximately 3 kg. Three 1-kg portions of this sample were transferred into a 5 l glass vessel. As leaching medium a mixture of chloride acid and nitric acid (aqua regia) was used. After the solutions were warmed up to approximately 90 °C, the pyrolised primary batteries were charged slowly and continuously. The solutions were stirred at about 300 rpm to accelerate the leaching process, after 24 hours the suspensions were hot filtrated and the filter cakes containing graphite and other not dissolved materials were submitted to XRF- and hot gas extraction analysis. The filtrate was analyzed by ICP on Zn, Mn, Fe, K, Cu, Ni, Al and Si. In Table 2 the results of these analyses are shown.

Table 2: Element contents of the investigated dry-pyrolised primary batteries [%]

Element	ZnO	MnO_2	Fe	C	K	Cu	Ni	Al	Si
Average content	31.4	31.1	27.3	5.6	3.3	1.1	0.2	0.1	0.2

Parallel three samples of the "black mass" (fine powder after mechanical beneficiation) were taken and analysed via AAS- and hot gas extraction analysis. The results are shown in table 3. As can be seen, the Mn/Zn-ratio varies from table 2 representing the variance of battery scrap mixtures treated in Europe.

Table 3: Element contents of the wet (non-pyrolised) "black mass"-powder [%]

Element	Zn	Mn	C	Cu	Fe	Si	Al
Average content	23.4	33.2	7.8	0.5	0.3	< 0.05	< 0.05

4.3 Experiments in DC-SAF furnaces

The concept of operating an EAF on DC current is not new. DC furnaces have several unique requirements over AC furnaces in addition to the obvious differences in electrical power supply. DC furnaces have only one electrode mast arm and a single graphite electrode. In the conducted experiments this electrode acts as the cathode. Thus the top of the furnace is much less cluttered for the DC case and in general has fewer components to maintain as compared to AC designs. Some of the early benefits achieved with DC operation included reduced electrode consumption (50 % lower than conventional AC), reduced voltage flicker (50 to 60 % of conventional AC operation) and reduced power consumption (5 to 10 % lower than AC). The DC furnace however requires a second electrode, in this case the anode, to close the electrical circuit. This anode is commonly referred to as the bottom electrode because it is located in the bottom of the furnace shell. Several different designs exist for the bottom electrode including metal pin electrodes with non-conductive refractories, billet electrodes, metal fin electrodes and conductive bottom refractory.

On the other hand, submerged arc furnaces (SAF) produce a wide range of metal products by smelting various minerals to metals products, in some processes a valuable slag or vapour product arises as well as the metal. The term SAF is used because the electrodes are usually buried deep in the furnace burden and the reduction reaction takes place near the tip of the electrodes. As the burden descends in the furnace the non-carbon portion of the charge begins to melt. As the carbon heats, its resistance decreases providing a conductivity path trough the charge. This current flow creates ohmic losses and thereby the intense heat needed for the high temperature and energy required for the reduction reactions. SAF-furnaces produce high-carbon ferromanganese typically 79 % Mn and 7 % C.

In the present work, several lab-scale experiments and semi-pilot-tests in DC-SAF's have been carried out. Preliminary different slag systems supposed to allow high manganese and zinc recovery from spent primary batteries were investigated theoretically and experimentally with a focus on metal–slag equilibria, see [4]. Afterwards suitable operation parameters and process conditions were determined and scaled-up from laboratory to semi-pilot-scale.

4.3.1 Lab-scale test

4.3.1.1 Equipment and experimental procedures

The used laboratory-scale DC-SAF operates at max. 96 kVA, the tapping capacity is about 10 kg steel, the inner size of the furnace is 0.5 m in height and 0.2 m in diameter; the electrodes used have a diameter of 50 mm. The refractory material was a ramming mixture based on MgO. The furnace is provided with a water-cooled bottom anode made of copper. The cathode's vertical position is adjustable by a hydraulic system. An exhaust gas system collects the off-gas and transfers it to a water-cooled spark separator and to a bag filter in which the flue dust is separated and collected. Temperatures of the furnace shell and of the copper electrode on different positions are continuously monitored by means of thermocouples connected to a computer. Figure 10 (left) shows the lab-scale DC-SAF at IME Aachen and Figure 10 (right) some details.

During charging the reduction reactions presented in chapter 2 occur. The battery's steel shell and the reduced manganese form a ferromanganese alloy in the bottom part of the furnace, while zinc oxide is reduced, evaporated, re-oxidized and collected in the bag-house system as a separate dust product (zinc oxide). The experimental and analytical procedure was defined as follows:

For pre-heating of the lab-furnace approx. 1 kg lignite coke is charged and heated. After 60 minutes heating time, the remaining ash is removed.

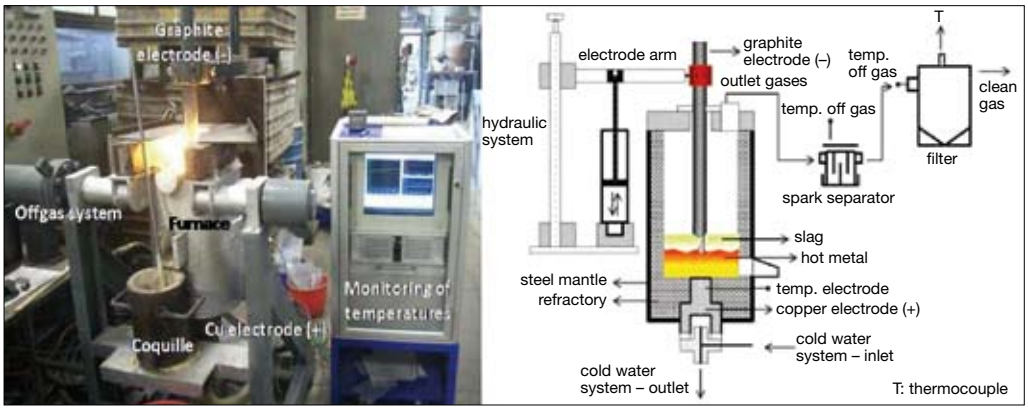

Fig. 10:
Laboratory scale DC-SAF at IME Aachen (left: view with data logging system; right: scheme of the installation)

For some experiments 3 kg of a FeMn-alloy with about 25 wt.-% Mn in form of small discs are charged and melted to form a pre-melt in order to simulate a continuous process with a remaining melt after tapping.

Half the amount of a homogenized synthetic slag is added and melted during approx. 20 minutes with the aid of the electric arc from the graphite electrode.

The temperature in the slag bath is measured manually with a thermocouple type lance.

A premix of pyrolised batteries and the corresponding mass of lignite, in some cases "black mass" pellets, and the second part of the synthetic slag are alternately and slowly charged into the furnace for about 30 minutes.

After complete melting the temperature is discontinuously measured during about half an hour until the temperature stays constant at about 1500 °C.

Metal and slag are tapped together into a pre-heated cylindrical steel mould.

After cooling slag and metallic phases are separated, weighed and sampled. The EAF-dust is taken out of the bag-house system, weighted and stored in a hermetic plastic bag for analysis (ICP, AAS). The slag is analysed for Mn, Ca, Si, Al, Mg, and Fe^{tot}. The metallic phase is analysed for Mn, Fe, C, Si and Cu, while the EAF-dust is analysed for Zn, Mn and Fe.

Table 4 presents the conducted laboratory-scale tests. The plan shows that in the first three experiments no starting slag was used, in exp. 4 to 6 a FeMn-alloy with approximately 25 wt.-% Mn was initially melted. All subsequent tests were conducted together with pelletised "black mass" in order to increase the Mn/Fe-ratio. Three different slag systems were tested, based on prior investigations (published here in January 2006): $CaO–SiO_2$, $CaO–SiO_2–Al_2O_3$ and $CaO–SiO_2–Al_2O_3–MgO$. Figure 11 shows the flowchart of the investigated process.

Table 4:
Experimental plan of the charged materials (laboratory-scale)

Heat Nr.	Pyrol. Batt. [g]	Pre-melt FeMn25 [g]	Black mass [g]	MnO_2/ Fe	Slag composition [wt.-%]				Amount of lignite [g]	Amount of slag [g]	Basicity*
					CaO	SiO_2	Al_2O_3	MgO			
1	6000	–	–	1.0	–	–	–	–	1220	–	–
2	6000	–	–	1.0	–	–	–	–	1220	–	–
3	6000	–	–	1.0	–	–	–	–	1220	–	–
4	3000	3000	–	0.7	56.3	43.7	–	–	611	300	1.29
5	3000	3000	–	0.7	46.7	38.3	15	–	611	300	0.88
6	3000	3000	–	0.7	45.7	37.3	14	3	611	300	0.95
7	6000	–	3000	1.9	56.3	43.7	–	–	1978	450	1.29
8	6000	–	3000	1.9	46.7	38.3	15	–	1978	450	0.88
9	6000	–	3000	1.9	45.7	37.3	14	3	1978	450	0.95
10	3000	–	3000	2.5	56.3	43.7	–	–	1380	300	1.29
11	3000	–	3000	2.5	46.7	38.3	15	–	1380	300	0.88
12	3000	–	3000	2.5	45.7	37.3	14	3	1380	300	0.95
13	3000	–	6000	3.8	56.3	43.7	–	–	1739	450	1.29
14	3000	–	6000	3.8	46.7	38.3	15	–	1739	450	0.88
15	3000	–	6000	3.8	45.7	37.3	14	3	1739	450	0.95
16	3000	–	6000	3.8	45.7	37.3	14	3	1739	450	0.95
17	3000	–	10000	5.4	56.3	43.7	–	–	2490	450	1.29
18	3000	–	10000	5.4	46.7	38.3	15	–	2490	450	0.88
19	3000	–	10000	5.4	45.7	37.3	14	3	2490	450	0.95
20	3000	–	10000	5.4	56.3	43.7	–	–	2490	450	1.29

*B = (% CaO + % MgO)/(% SiO_2 + % Al_2O_3)

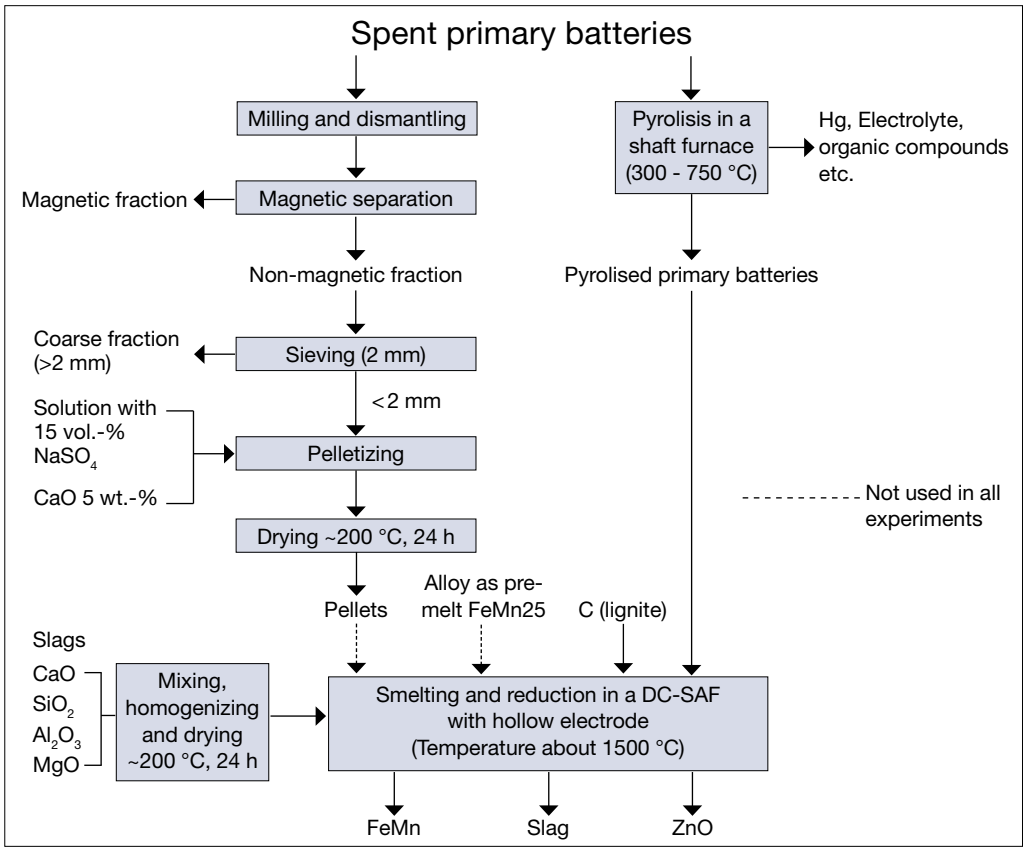

Fig. 11:
Flowchart of the investigated process to recycle spent primary batteries in a DC-SAF-process

4.3.1.2 Results of SAF-batch laboratory-scale experiments

The results of the laboratory-scale experiments were useful to analyze the effect of different variables in the DC-SAF-process. These results will not be discussed in detail because they were designed to find the most important parameters to be implemented in the follow experimental phase (semi-pilot experiments).

4.3.1.3 Products from laboratory-scale experiments

Table 5 shows the chemical composition of the obtained products (alloy, slag and flue dust) from the laboratory-

Heat	Fe-Mn alloy [wt.-%]						Slag [wt.-%]					Flue dust [wt.-%]		
Nr.	Mn	Fe	Si	Cu	C	Mn/Fe	Mn	Ca	Si	Al	Mg	Zn	Mn	Fe
1	14.9	78.7	0.3	3.2	2.9	0.2	46.4	–	–	–	–	29.8	29.7	–
2	2.5	90.2	0.2	5.6	1.5	0.03	57.5	–	–	–	–	30.4	30.3	–
3	4.8	86.6	0.2	6.2	2.2	0.1	55.5	–	–	–	–	31.0	29.4	–
4	33.8	58.7	–	3.2	4.3	0.6	41.5	3.9	10.2	–	0.5	17.5	10.5	12.1
5	34.5	57.3	–	3.7	4.5	0.6	45.9	3.9	4.2	–	–	22.6	12.2	10.5
6	36.2	55.5	–	3.8	4.5	0.7	46.1	4.5	4.5	4.7	4.1	21.0	11.6	11.4
7	20.6	71.2	0.3	3.6	3.8	0.3	41.5	4.2	9.6	–	–	39.5	14.8	1.3
8	19.7	75.1	–	1.5	3.7	0.3	46.0	2.1	–	–	0.6	43.8	10.2	0.9
9	21.3	69.4	0.3	3.2	3.7	0.3	49.5	4.5	5.8	1.3	4.7	45.0	5.0	0.9
10	27.2	67.5	0.2	2.1	3.0	0.4	61.0	2.1	1.9	1.0	0.9	43.0	7.2	0.8
11	26.3	65.7	0.3	3.7	4.0	0.4	49.5	4.2	9.7	1.1	0.6	34.3	11.0	1.5
12	27.5	66.9	0.3	1.5	3.8	0.4	53.2	1.7	5.2	0.6	0.8	46.2	9.5	0.9
13	29.1	61.3	0.3	4.7	4.6	0.5	27.2	6.8	6.4	6.4	8.2	48.7	9.6	0.3
14	29.5	64.9	0.3	1.9	3.4	0.5	58.2	2.9	1.5	2.7	1.1	33.2	12.4	1.7
15	30.8	63.1	0.2	2.1	3.8	0.5	48.6	3.5	5.9	5.0	2.0	41.3	11.9	1.6
16	36.3	57.7	0.1	2.2	3.7	0.6	50.5	2.3	4.7	6.5	3.0	45.9	7.6	0.7
17	32.2	61.8	0.2	3.1	2.7	0.5	52.0	3.7	1.9	0.6	2.1	38.4	14.0	1.1
18	33.8	58.6	0.3	2.5	4.8	0.6	38.8	6.9	9.9	4.4	1.7	41.0	7.1	0.8
19	35.7	56.5	0.1	2.2	5.5	0.6	24.6	3.8	–	–	8.5	41.0	13.2	1.1
20	37.7	53.9	0.1	2.7	5.6	0.7	43.9	1.5	7.1	5.0	3.1	39.3	1.0	1.0

Table 5:
Chemical composition of the products: alloy, slag and flue dust (laboratory-scale experiments)

scale experiments. For the metallic products, the ratio between manganese and iron is also shown.

In all experimental tests, the content of zinc in the slag phase was found in values lower than 0.1 wt.-% and in the metallic phase the concentrations were practically zero. Based on this fact, it could be assumed that the zinc is totally evaporated, leaving the furnace as zinc-gas.

Experimentally in the tested laboratory scale trials, the concentration of carbon in the alloy was found a key parameter to make the recovery of manganese from the slag to the alloy possible, the effect of the manganese concentration in the metallic phase as function of the carbon content in the alloy is shown in Figure 12 and the concentration of manganese in the slag phase as function of the carbon content in the alloy is shown in Figure 13. At between 1 wt.-% and 2 wt.-% carbon in the alloy, the manganese-content in the slag remains very high (concentration of about 60 %), as the concentration of carbon in the alloy increases, the reduction of manganese from the slag increases with the corresponding considerable increment of manganese in the alloy. Lower contents of manganese in the slag (values of about 20 %) were found at contents of about 6 to 7 wt.-% carbon in the alloy leading to recoveries higher than 50 wt.-% manganese in the alloy.

Figure 14 shows the effect of the experimental basicity values of the slag on the final manganese-concentration in the slag phase. As the basicity values increases, the manganese-content in the slag phase also decreases. The lowest content of manganese in the slag phase (about 25 wt.-%) has been achieved between B-values of 1.0 and 1.3.

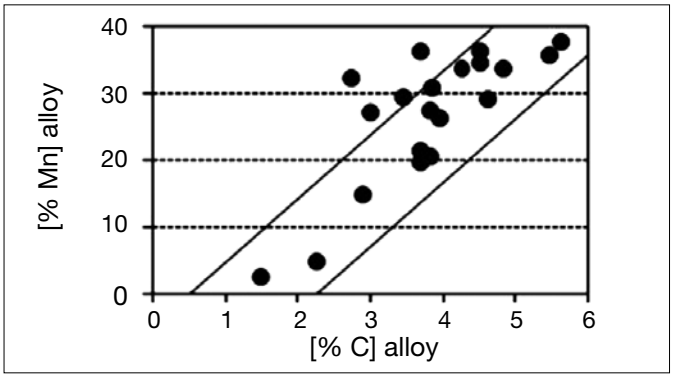

Fig. 12: Effect of the [% C]-alloy in the content of Mn in the metallic phase

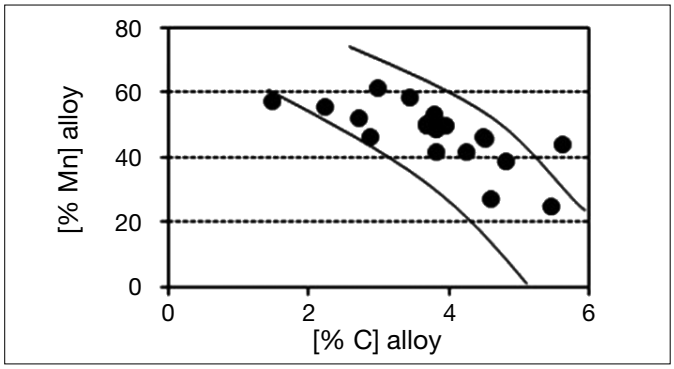

Fig. 13: Effect of the [% C]-alloy in the content of Mn in the slag phase

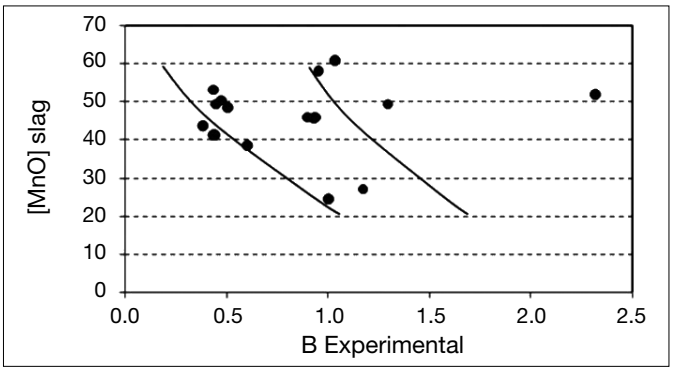

Fig. 14: Manganese concentration in the slag phase as function of the experimental basicity B

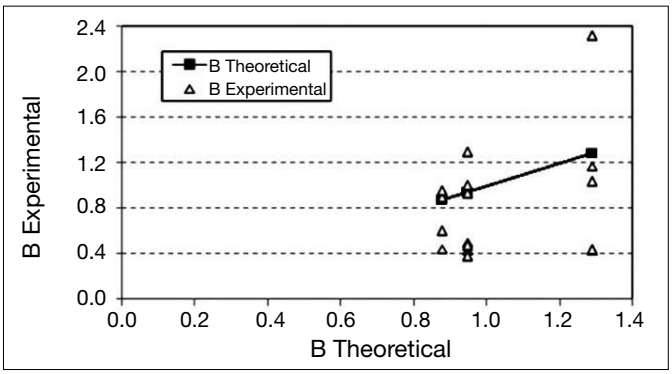

Fig. 15: Comparison between theoretical and experimental values of basicity for the laboratory scale EAF-experiments

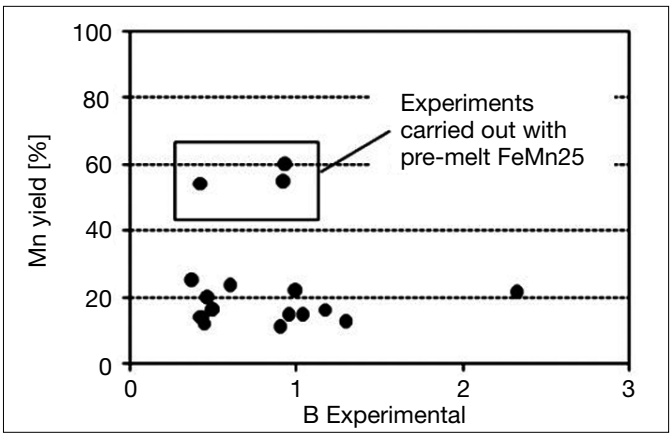

Fig. 16: Manganese yield as function of the basicity

Experimentally it was difficult to keep the theoretical expected basicity of the process. Figure 15 shows a comparison between the theoretical expected basicity values and the final experimental obtained basicity values.

Figure 16 shows the Manganese yield (in the ferromanganese alloy) as function of the experimental basicity. The highest recovery-yield values (approximately 60 %) have been obtained at a basicity value of 1 and with pre-melt (FeMn25).

4.3.2 EAF-semi-pilot scale experiments

4.3.2.1 Equipment and experimental procedures

The semi-pilot trials were run according to the best results and the determined operational process parameters that

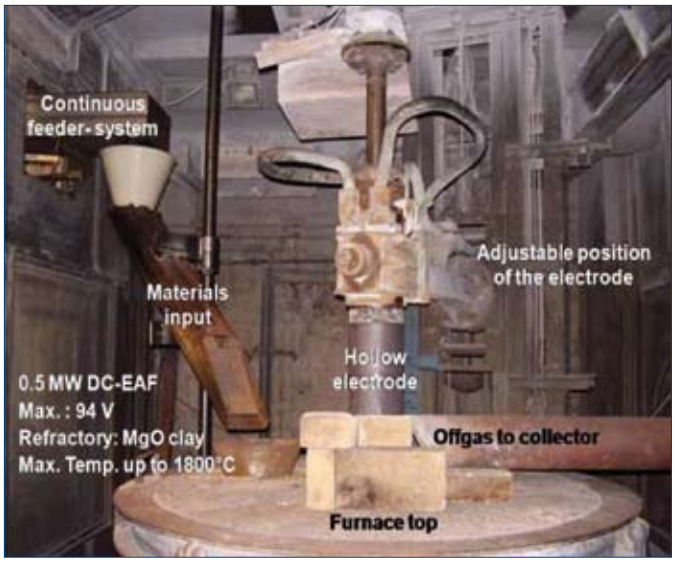

Fig. 17: Semi-pilot DC-EAF with hollow electrode at IME Aachen University

have been observed and concluded from the laboratory-scale experiments.

The semi-pilot scale arc furnace at IME Aachen (Figure 17) has an operational power rating of approximately 0.5 MWh. The furnace is provided with a water-cooled bottom anode of copper and a hollow graphite top-electrode, the vertical position of which is adjustable by an electrical system. The hollow electrode system for charging coke into the furnace has been developed at IME. An exhaust gas system collects the off gas and leads it to a spark separator and a bag filter, where the flue dust is separated. The inlet- and outlet-temperatures of the cooling water, various temperatures at different positions of the bottom electrode and the off gas system are continuously monitored. The refractory of the furnace was base on a MgO ramming mixture. The charging of the materials was done by means of a computer controlled feeder-system with an attached electronic balance at a rate of 80 kg/h.

The furnace was preheated with 200 kg of steel; the molten steel was tapped after two hours preheating time. The experimental procedure in the semi-pilot DC-EAF was homologous to the laboratory scale trials. During the process, the temperature of the melt was measured discontinuously about each 20 minutes by means of a thermocouple type lance. The experiments 21 and 22 were carried out with the hollow-electrode technique, while experiments 23 and 24 were done with full-electrode technique. In the former cases the hollow electrode was used for charging the lignite coke directly into the melt, whereas in the latter cases the coke was mixed with the input materials. Table 6 gives the materials charged and slag composition of the semi pilot experiments.

4.3.2.2 Results of SAF-semi-pilot-scale experiments

In this paper the results of the semi-pilot experiment will be shown and discussed in more detail than the laboratory-scale because they were designed according to the best process-parameters observed and concluded from these laboratory-scale experiments, and represent a pre-stage for an industrial scale-process.

4.3.2.3 Products from semi-pilot-scale experiments

In Table 7 to Table 9 the weights and the chemical composition of the products, tapping temperatures, the Mn and Fe yields, the Mn/Fe ratio in the alloy and the Mn distribution between slag and alloy are summarised corresponding to the pilot-scale experiments.

The calculations of Mn and Fe-yields were carried out taking into account the maximal concentration of Fe and Mn

Table 7: Weight of the products and tapping temperatures (semi-pilot scale experiments)

Heat Nr.	Products [kg]			Tapping temperature
	Fe-Mn-Alloy	Slag	Flue dust	[°C]
21	155*	73	32	1587
22	118*	59	26	1560
23	79	46	60	1562
24	77	45	70	1545

*Experiments carried out with pre-melt of 100 kg $FeMn_3O$

Heat Nr.	Pyrol Batt. [kg]	Pre-melt [kg]	Pellets [kg]	Slag [wt.-%] CaO	SiO_2	Al_2O_3	MgO	MnO/Fe	Lignite [kg]	used slag [kg]	Initial basicity
21	152	100*	–	10**	17**	5**	10**	0.6	30	60	0.9
22	138	100*	–	10**	17**	5**	10**	0.6	26	30	0.9
23	200	–	100	56	44	–	–	2.4	60	30	1.3
24	200	–	100	46	37	14	3	2.4	60	30	1.0

* The wt.-% Mn in FeMn-alloy used as pre-melted bath was about 30 wt.-% Mn.

** The slag from the industry has approximately the following composition in wt.-%: CaO – 10, SiO_2 – 17, Al_2O_3 – 5, MgO – 10, MnO – 50 and FeO – 2.

Table 6: Input materials and slag compositions (semi-pilot scale experiments)

Heat	Alloy					Slag						Flue dust		
Nr.	Mn	Fe	Si	Cu	C	Mn	Ca	Mg	Si	Al	Fe	Zn	Mn	Fe
21	37.9	55.5	0.3	2.7	3.6	34.6	3.7	4.7	–	–	2.0	54.8	6.2	–
22	45.6	47.2	0.3	2.4	4.5	24.6	6.1	7.8	–	–	14.0	40.8	24.9	–
23	47.7	45.3	0.8	1.3	4.9	32.1	7.3	–	6.5	–	2.0	41.0	13.2	1.1
24	52.2	36.8	1.9	3.1	5.8	22.4	15.1	3.8	4.5	7.4	0.3	52.0	23.0	15.0

Table 8: Chemical composition of the products: alloy, slag and flue dust (semi-pilot scale experiments) [wt.-%]

Table 9: Mn and Fe yield and ratios Mn_{slag}/Mn_{alloy} and Mn_{alloy}/Fe_{alloy} (semi-pilot scale experiments)

Heat Nr.	Mn yield [%]	Fe yield [%]	Mn_{slag}/Mn_{alloy}	Mn_{alloy}/Fe_{alloy}
21	*60.8	*67.6	0.43	0.70
22	*55.4	*-12.3	0.27	1.00
23	39.5	70.2	0.40	1.10
24	42.1	55.5	0.25	1.40

* The values from experiments 21 and 22 were calculated without the pre-melt

in the ferroalloy from the industry (60 and 30 wt.-% respectively) used in the experiments 21 and 22 as pre-melt. For this reason and because of the strong chemical composition variation of the pyrolised spent primary batteries a negative yield from Fe in experiment 22 was found.

Figure 18 shows the theoretical and experimental ratios between Mn and Fe in the final alloy (left) and indicates the effect of the carbon content in the final alloy on the silicon content in the alloy (right). In the experiments 21 and 22 the ratio Mn/Fe was a bit higher than expected because of the use of the pre-melt. In experiments 23 and 24 the Mn/Fe ratio was lower than expected, this can be attributed to an incomplete reduction of manganese oxides presented in the pyrolised primary batteries as well as in the black mass. On the other hand as the concentration of carbon in the final alloy increases, the partial reduction of silica from the slag takes place generating metallic silicon in the alloy.

Figure 19 shows the effect of the C-content in the alloy on the Mn-content in the alloy (left) and on the Mn-content in the slag (right) for the pilot experiments. As the concentration of C in the alloy increases, the concentration of Mn in the alloy increases with the corresponding decrement of the Mn concentration in the slag phase. This effect of the carbon content in the alloy on the reduction of Mn from the slag has been expected from the thermo-chemical modelling in the software FactSage.

Figure 20 shows the effect of the CaO content in the final slag on the Mn content in the alloy (left) and on the Mn content in the slag (right). One more time the CaO content helps to keep a high basicity in the slag and has a positive influence on the reduction of MnO from the slag to the alloy.

In all experimental tests, the content of Zn in the slag phase was found in values lower than 0.1 wt.-% and in the metallic phase the concentrations were practically zero. Based on this fact, it can be assumed that the Zn is totally evaporated, leaving the furnace as Zn gas.

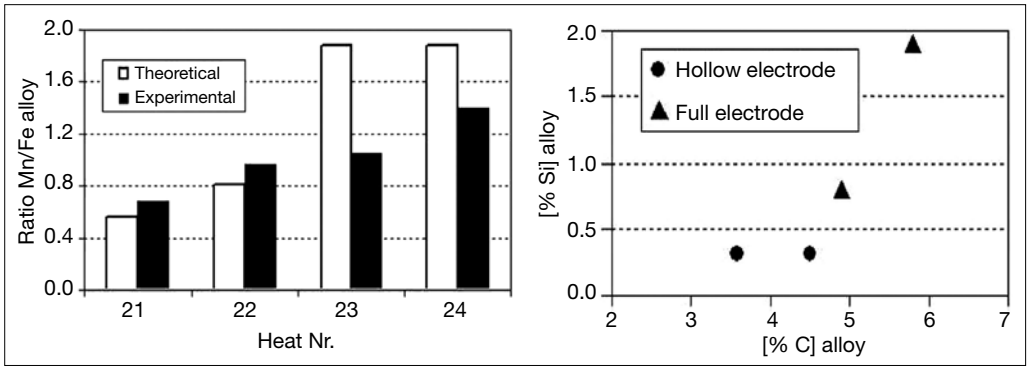

Fig. 18:
Theoretical and experimental Mn/Fe ratios in the Fe-Mn alloy (left) and the effect of % C in the alloy on % Si in the alloy (right)

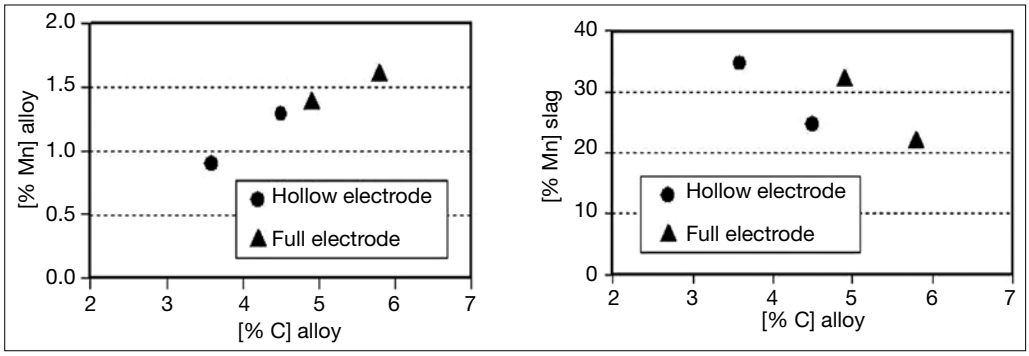

Fig. 19:
Effect of % C contained in the alloy on % Mn in the alloy (left) and on % Mn in the slag (right)

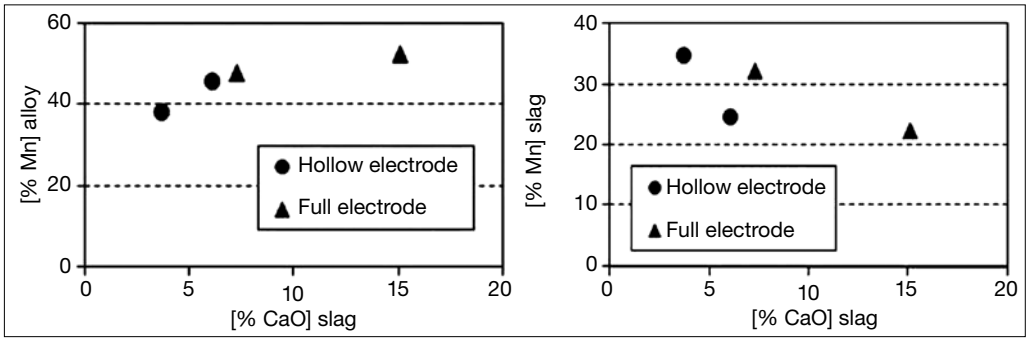

Fig. 20:
Effect of % CaO in the slag on % Mn in the alloy (left) and on % Mn in the slag (right)

Fig. 21:
Fe-Mn slab from (left) and flue dust (right) from a semi-pilot scale experiment

During the process the smelting temperature has been measured with a lance thermocouple; the temperature of the slag and alloy in the submerged arc process was constantly approximately 1550 °C. At this temperature practically all the FeO was found to be converted to iron, therefore experimentally very low concentrations on iron in the slag at the end of the process were found; however, the extent of the conversion of MnO to manganese varied greatly since Mn is much more ignoble than iron. Figure 21 shows the produced Fe-Mn alloy (left) and the flue dust (right) obtained after a trial.

The trials that used industrial slag (experiments 21 and 22) showed a high viscosity of the slag, even at temperatures higher than 1600 °C. This can be attributed to the relatively high MgO content.

5 Summary and conclusions

This paper discusses the feasibility and applicability of the submerged arc furnace technology for the reprocessing of spent primary batteries using a carbothermic process.

In the reprocessing of spent primary batteries in the submerged arc furnace there are many reactions taking place simultaneously. Computational thermodynamics is a convenient way of modelling smelting in order both to better understand the process and to explore the effect of changing process variables on the outcomes. The software FactSage 5.3.1 was used in this work for modelling submerged arc smelting for the production of ferromanganese and zinc oxide from pyrolised respectively beneficiated spent primary batteries.

A DC-SAF process was designed, tested and optimised. Several laboratory scale experiments were useful to fix the most important process parameters for a semi-pilot-scale process to produce ferromanganese and a zinc oxide-concentrate in a single step process.

The MnO_2-reduction mechanism begins with the increase of the furnace's temperature. The MnO_2 dissociation occurs either with carbon or gaseous CO produced in the furnaces because of the combustion of C from charged lignite coke, the furnace's graphite electrode, and the graphite contained in the spent primary batteries. The partial reduction of manganese oxides liberates oxygen as a product of the decomposition according to (3), (4) and (5) and thereby increasing the furnace's temperature because of the promotion of the combustion of carbon. Mn^{2+} as MnO is the lowest manganese oxide; during the process this oxide is present in the molten slag, from where the metallization of manganese is possible. The reduction of MnO takes place between the metal–slag interface and is only possible under stronger reductive conditions and at higher temperature of at least 1400 °C. The steel shell of the spent primary batteries is directly molten forming a molten bath in the bottom of the furnace. Carbon is dissolved in the molten bath and having contact with the C-saturated MnO slag, the reduction of MnO takes place and the formation of ferromanganese together with manganese carbides appears. Any formed iron oxides in the slag will be reduced easily and almost completely to metallic iron during smelting whereas the manganese oxides require much stronger reductive conditions and the recovery of manganese could not be complete.

The reduction of zinc oxide takes place above the surface of the liquid bath (slag and metal). Based on assumptions (11), (12) and (13), zinc oxide is first reduced and then evaporated at temperatures about 900 °C. Between 1100 and 1300 °C zinc oxide is completely reduced by the presence of carbon monoxide which is produced by the combustion of the added carbon, furnace's graphite electrode and graphite from the spent batteries, accompanied by the Boudouard reaction to renew the carbon monoxide. Subsequently the metallic gaseous zinc is quickly re-oxidized by the oxygen contained in the secondary air in the off gas. The re-oxidized zinc settles as dust in the bag house system.

The carbon content in the final Fe-Mn alloy is a key parameter as well as the relative high calcium oxide content in the slag phase to achieve high manganese recovery values. However the content of carbon in the alloy should not be higher than 6 wt.-%, otherwise the concentration of silicon (from the partial-reduction of the silica) overcomes for example the industrial requirements of "high carbure Fe-Mn" (where a maximum of 1.25 wt.-% silicon in the alloy is allowed). With CaO contents higher than 17 wt.-% in the slag phase, the conduction of the process was quite difficult because of high viscosity of the slag.

The hollow-electrode technique showed good possibilities to be implemented in the reprocessing of spent primary batteries leading to satisfactory recovery values, reaching high metallic recoveries that can be compared to the

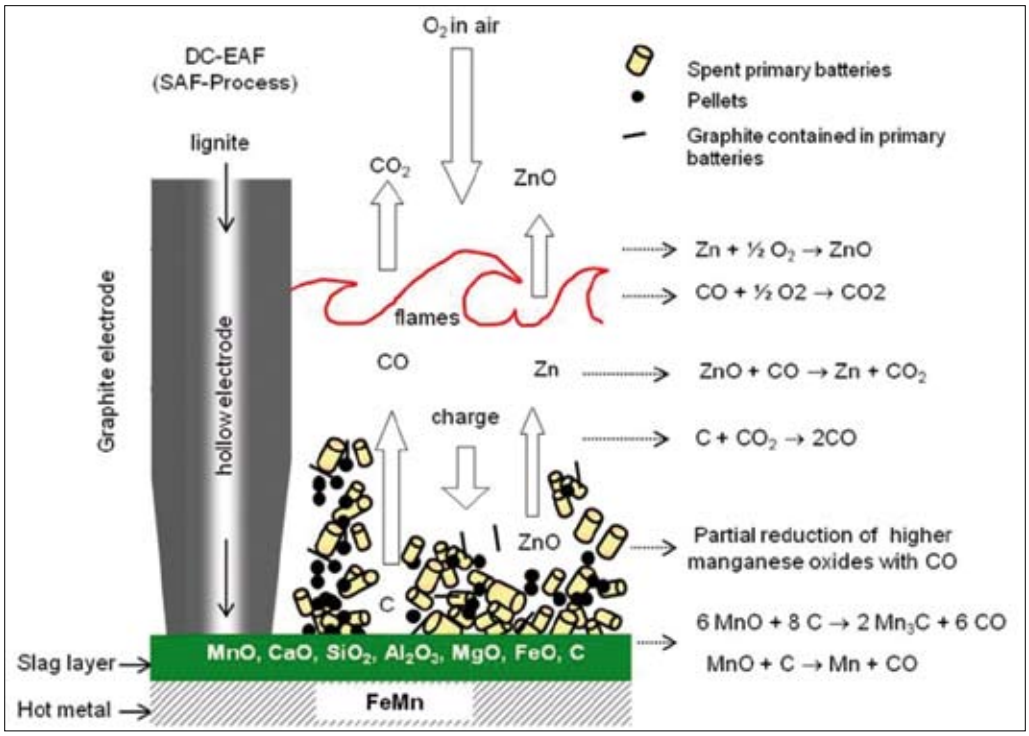

Fig. 22:
Reactions mechanismus during the treatment of primary batteries in a DC-SAF process

full-electrode route. A comparative analysis of these two possible techniques should be done in more detail in order to estimate and evaluate different important parameters in the process such as graphite and energy efficiency, technical feasibility, processing time, etc.

The above mentioned most probable and important reactions which take place in the investigated process for the reprocessing of pyrolised spent primary batteries (DC-SAF process) are illustrated in Figure 22.

Three different slag systems were tested with full- and hollow-electrode technique, allowing recovery values of: Mn between 44 and 62 %, Fe between 56 and 96 % and Zn apparently around 100 % (because practically no Zn was found in the slag and in the metallic phase).

The experimental recycling quotas (see Figure 23 standardized values to 100 % from exp. 23) were found very close to the theoretical expected calculated values for Mn, Fe and Zn from the recycling of pyrolised spent primary batteries

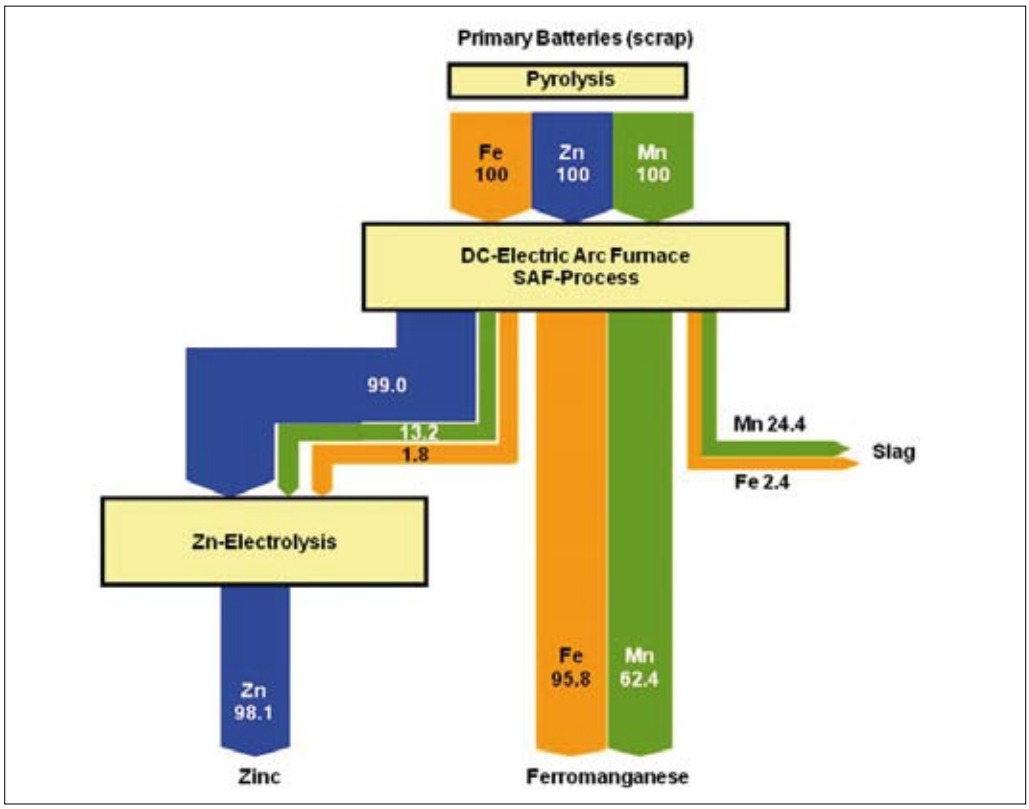

Fig. 23:
Flow of the metals in the course of the reprocessing of spent primary batteries through the DC Submerged Arc Furnace technology (standardized values to 100 % from exp. 23)

in a SAF process (see chapter 1.2.3). In the metallic phase Mn was expected up to 66 wt.-% but experimentally was found 62.4 wt.-%. For iron was expected 88.4 wt.-% in the alloy and experimentally was reached 95.8 wt.-%. In the slag phase, Mn was expected 15 wt.-%, however 24.4 wt.-% was found. Iron has been expected 11.5 wt.-% in the slag phase, nevertheless only a 2.4 wt.-% was found. In the flue dust, Mn was theoretically expected 19 wt.-%, experimentally was reached a value of 13.2 wt.-%. The theoretical and experimental values for Zn in the flue dust were identical (practically 100 wt.-%).

Acknowledgment

The authors are grateful to the DBU Deutsche Bundesstiftung Umwelt, to the German Academic Exchange Service, DAAD, as well as to the Mexican Council for Science and Technology, CONACyT, for financial support of the experimental research part. The authors want to acknowledge the personal support from Mr. A. Krebs (Batrec AG, Swiss) and Mr. M. Berger (Redux GmbH, Germany) for their cooperation in this work.

Literatur

[1] Recyclingrekord bei Batterien (2006): Sekundäre Rohstoffe, **23**: 157.

[2] INOBAT und GRS Batterien (1994-2007)

[3] Muth, A. (oder B. ???)(1996): Daten und Fakten zum Umweltschutz: pp. 18-19; Springer.

[4] Sanchez, R. & Friedrich, B. (2007): Optimization of the Ferromanganese Production from Spent Primary Batteries-Design of the Process Slag. – ERZMETALL, **60**: 7-14.

[5] Brooks, C.S. (1986): Metal recovery from industrial wastes. – Journal of Metals, **38**: 50-57.

[6] Rombach, E.; Friedrich, B. & Berger, M. (2006): Recycling efficiency of the reprocessing of primary batteries: International Conference of Battery Recycling ICBR 2006, Interlaken, Swiss.

[7] Riss, M. & Khodorovsky, **(X)???**(1964): Production of ferroalloys: pp. 135-158. Moscow (Foreign Languages Publishing House). pp. 135-158.

[8] Hooper, R.T. (1968): The production of Ferromanganese. Journal of Metals. **20**: 88-92.

[9] Biswas, A.K. (1981): Principle of Blast Furnace Ironmaking: 72-81, 87-91. Brisbane (Cootha Publ. House).

[10] Pausteri, J.F.; Bounds, C.O. & Lherbier, L.W. (1998): Journal of Metals, **50**: 31-35. **(Aufsatztitel fehlt)**

[11] Bale, C.W. & Pelton, A.D. (1990): The Unified Interaction Parameter Formalism: Thermodynamic Consistency and Applications. – Metall. Trans. Act. **21A**: 1997.

[12] Lupis, C.P. & Elliott, J.F. (1966): Generalized Interaction Coefficients: Part I: Definitions. – Acta Metall, 14: 529-538.

[13] Eriksson, G. et al. (1994): Critical Evaluation and Optimization of the Thermodynamic Properties and Phase Diagrams of the MnO-S. Canad. Met. Quart. **33**: 13-21.

MSc. Ricardo Sánchez-Alvarado
Prof. Dr.-Ing. Bernd Friedrich
Both:
IME Process Metallurgy and Metal Recycling
Department and Chair of RWTH Aachen University
Intzestrasse 3
52072 Aachen
Germany